

RADAR-BASED URBAN DETECTION OF GREATER COCHIN DEVELOPMENT AREA (GCDA), THE QUEEN OF ARABIAN SEA, KERALA, INDIA

Sumith Satheendran S.

Amrita-Natural Resource Monitoring Laboratory (Amrita-NRML), Earth Observation Group, Amrita School of Physical Sciences, Department of Chemistry, Amrita Vishwa Vidyapeetham (Deemed University), Amritapuri Campus, Kollam-690525, Kerala, India

ABSTRACT

The urban dynamic temporal analysis involves systematically examining and interpreting spatiotemporal patterns in urban environments, enabling a deeper understanding of how cities evolve and informing decision-making processes for sustainable urban development. Using remote sensing is essential for the investigation of urban dynamic temporal changes by providing a comprehensive and detailed understanding of urban landscapes over time. This study utilizes Synthetic Aperture Radar (SAR) satellite imagery acquired from the Sentinel mission to investigate the detection of urbanization changes within Kochi, a rapidly expanding metropolitan region in India, between 2015 to 2023. The urban footprint was calculated using a change detection technique that relies on supervised classification and was applied to SAR data. Both training sites and ground truth points (150) were used to estimate the accuracy assessment. The results of the analysis revealed a significant increase in urban expansion in Kochi, as indicated by the data. In contrast to alternative methods, the Speckle Divergence technique applied to Vertical-Vertical (VV) and Vertical-Horizontal (VH) polarizations demonstrates enhanced precision in identifying urban areas. The analysis accuracy results showed that the study's data and methodology could be used to determine the urban footprints efficiently.

ARTICLE HISTORY

Received: 31 May 2024

Revised: 8 June 2024

Accepted: 9 June 2024

KEYWORDS

Urban dynamics

SAR

Speckle Divergence

Sentinel-1

Polarizations

1. INTRODUCTION

Urban expansion is the process by which cities spread out and harm ecosystems that are vital to the planet's well-being and continued existence. Constant rural migration into urban settlements/centers leads to overcrowding, which strains rehabilitation services. The trend of more people relocating to metropolitan areas is known as urbanization. People shifting from rural to urban areas, which increases the number of urban residents and the size of urban areas, is the main cause of it. Employing remote sensing to map urban environments and their development dynamics across diverse temporal and

spatial dimensions is a well-established practice (Li et al., 2020; Prakash et al., 2023; Wang et al., 2019). The emergence of Synthetic Aperture Radar (SAR) technology has significantly expanded the possibilities for monitoring urban areas, owing to its capability to detect and analyze the polarimetric characteristics of both artificial structures and natural scattering elements (Yamaguchi et al., 2005). Research findings indicate the identification of urban environments through the utilization of speckle divergence analysis. This method effectively accentuates regions distinguished by diverse and extensively organized built-up segments (Esch et al., 2009; Thiel et al., 2008). The technique of Persistent Scatterer Interferometry

*Corresponding author. Email: remotesumithsat@gmail.com

Synthetic Aperture (PSInSAR) presents an advanced form of Differential Interferometry Synthetic Aperture Radar (DSInSAR) technology. It excels in identifying and tracking changes in Earth's surface dynamics across temporal intervals. This methodology amalgamates a series of SAR images taken over time, enabling the detection and measurement of delicate surface shifts (subsidence or uplift) on various scales, spanning from local to regional. Central to this approach are coherent and enduring radar reflectors referred to as Persistent Scatterers (PS), which predominantly encompass steady radar responses over extended periods. These scatterers often manifest as either artificial structures or natural elements (Wang et al., 2022).

In the recent years, change detection methods have extensively utilized remote sensing information. The presence of remote sensing data enhances both the caliber and quantity of observing and assessing the progression of urbanization (Alharthi et al., 2020). The precision of spatial accuracy can vary in urban expansion scenarios (Bahrawi et al., 2020). Altering the configuration of the Earth's surface could potentially result in catastrophic events, especially if there are significant modifications to the morphological features of a specific region (Elhag et al., 2013; Massonnet and Feigl, 1998; Schumm, 1979) utilized SAR and ERS datasets to observe the process of urbanization. Esch et al. (2009) explored a method for the semi-automated identification of urbanized regions using single polarized TSX images, with a specific emphasis on analyzing speckle characteristics. Taubenböck et al. (2012) examined the urban expansion of 27 megacities through the utilization of Landsat and TerraSAR-X. SAR imagery finds its predominant applications in the ecological oversight of land-based settings. This investigation leverages SAR satellite images sourced from the Sentinel missions to scrutinize the progression of urbanization and alteration in Land Use and Land Cover (LULC) within Kochi, a rapidly expanding metropolitan expanse in India, spanning the temporal span from 2015 to 2023.

2. METHODOLOGY

2.1. Study area

The Greater Cochin Development Authority (GCDA) is in charge of the metropolitan area of Kochi's planning and development. The GCDA's jurisdictional area includes Kochi City, Kerala's com-

mercial hub, Kochi Corporation, nine neighbouring municipalities, and 21 intervening panchayats, a total of 632 sq.km (May and Jose, 2009). A port city with a population of around 2.1 million, Kochi is situated at 10°N and 76°E on the southwestern coast of India. Greater Kochi includes the remainder of the Cochin Peninsular, British-made Wellington Island, other islands west of the mainland, and a sizable portion of the mainland of Ernakulum (Satheendran et al., 2022). In the preceding three decades, Kochi has experienced swift population expansion. According to the 2001 census data, the population of Kochi was 596473 (Shreekumar et al., 2021). The urban areas are crisscrossed by estuaries nourished by continuous inflows from rivers. A significant portion of Kochi is situated at the same altitude as the sea. The climate of Kochi showcases a tropical monsoon pattern (Thomas et al., 2014). An illustrative depiction of the research site is presented in Fig. 1.

2.2. Sentinel-1 data sets

The Sentinel-1 sensor was created to operate in the electromagnetic spectrum's microwave region. Based on S1A and S1B instruments, Sentinel-1 delivers multi-temporal SAR data with a temporal resolution of 12 days. Sentinel-1A is made to take four different acquisitions in the C-band (4.0-8.0 GHz) to image the electromagnetic spectrum. Sentinel-1 is a collection of radiometrically calibrated, thermally noise-corrected, and geometrically terrain-corrected SAR satellite images. The products made by Sentinel-1 are either single-polarized or dual-polarized. Vertical transmit/vertical receive, or HH (Horizontal transmit/Horizontal receive), are the two possible single-polarized products. Similar to this, dual-polarized products can be polarized as "HH+HV" (Horizontal transmit/Horizontal receive and horizontal transmit/vertical receive) or "VV+VH" (Vertical transmit/Vertical receive and Vertical transmit/Horizontal receive). The pixels used to create the images are roughly square (10 m × 10 m). Information regarding the utilized Sentinel-1 image for research was presented in Table 1.

2.3. SAR Data Processing

The data preparation included image filtering, terrain correction, geometric correction, and speckle divergence SAR data. Subsequently, a fusion of Google Earth and Sentinel-1 data was executed to generate a sub-image, possessing a spatial resolution

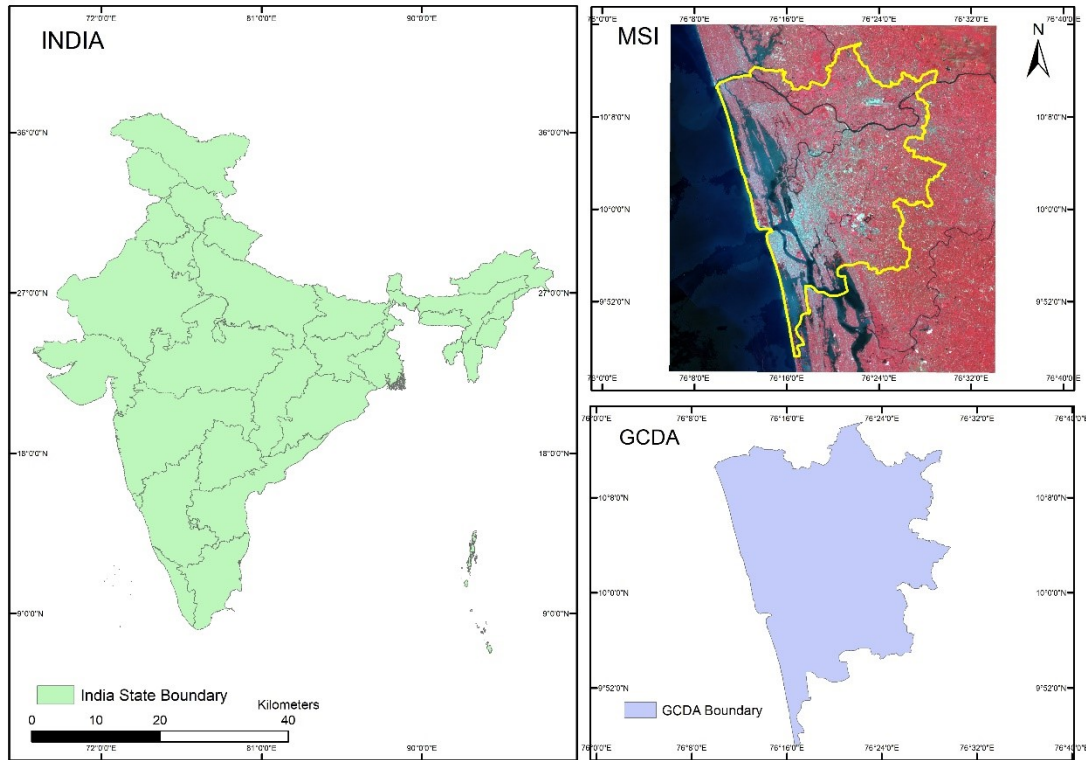


Fig. 1. Greater Cochin Development Authority (GCDA), Kochi Area.

Table 1. Description of the SAR products used in the project.

Satellite Product	Date of Acquisition	Spatial Resolution	Temporal Resolution
Sentinel-1 log-scaled SAR	Mean image from image collection (2015-02-26)	10 m	12 days
Sentinel-1 log-scaled SAR	Mean image from image collection (2023-02-20)	10 m	12 days

of 10 m. The Sentinel Application Platform (SNAP) software was then used for atmospheric correction, picture mosaicking, multi-look processing, SAR data filtering, and geometric correction. The polarized SAR image underwent resampling to a 10 m resolution using the nearest-neighbour resampling technique. Resampling was performed to facilitate the integration of optical imagery with the SAR datasets. Owing to inherent geometric imprecision and the impact of atmospheric conditions, it is imperative to undertake radiometric and geometric correction on SAR imagery prior to its applications, ensuring utmost precision. When employing single-data or multi-data images for classification purposes, the utilization of Ground Control Points (GCP) facilitates the achievement of geometric accuracy, thereby elucidating the necessity for radiometric rectification. While an individual-dated image may bypass atmospheric adjustments, the significance of radiometric correction becomes pronounced when categorizing photographs from diverse temporal instances.

The primary emphasis of this study revolves around Level-1 ground range detected data acquired via the Interferometric Wide swath products, representing the standard data collection method over terrestrial regions. The source imagery for this research is from the Sentinel’s Scientific Data Hub, an openly accessible resource for scientific study. The collection encompasses both the original satellite imagery and their radiometrically calibrated duplicates. It is noteworthy that the radar backscattering from the Earth’s surface exhibits a direct correlation with the pixel values found in data that has undergone radiometric certification. The calibrated edition of the SAR data becomes imperative for quantitative applications, contrasting with the qualitative utilization of the initial SAR data. The calibration of radiometric SAR visuals was executed through the utilization of the SNAP program. In this study, GeoTIFF format images were employed for both the raw data and its corresponding calibrated iteration. The process of directly and professionally annotating SAR images is an

intricate and time-intensive undertaking. Moreover, the relatively subpar quality of the images renders the task of identifying the target category exceedingly arduous. A potential solution to these challenges arises from utilizing optical images sourced from the Google Earth Engine, which effectively narrows the gap between radar's active imaging modes. In the context of this, human observation swiftly identifies optical images, leading to precise annotations.

The present research involves an analysis of two distinct Sentinel-1A SAR images: one captured on February 26, 2015, and another on February 20, 2023. Subsequently, the orbit file and the Sentinel-1A image are inputted into SNAP jointly. To convert the intensity measurements from the Sentinel-1A image into sigma naught, a radiometric calibration technique is applied. The geographical scope of interest, represented by the GCDA, is applied to both sets of Sentinel-1 SAR data. This step includes terrain flattening and geometric adjustment to align with the study region accurately. Essential data for implementing the calibration equation are integrated within the Sentinel-1 Ground Range Detected (GRD) product. The process involves executing radiometric calibration and selecting the newly generated orbit file from the source product dropdown menu within the input-output parameters. It is important to note that ongoing processes do not propagate speckle. Therefore, caution is advised against applying speckle filtering when identifying minor spatial features or preserving image texture is crucial.

Among various single-product speckle filters, the refined Lee filter outperforms others in terms of visual interpretation due to its ability to maintain edges, linear characteristics, point targets, and texture details. To mitigate these distortions and achieve a geometric representation of the image closely resembling reality, terrain corrections are essential. In this study, the Range-Doppler terrain correction method is employed. SNAP offers the Range-Doppler terrain correction operator, implementing the necessary adjustments.

Ortho-rectification techniques for geocoding SAR scenes acquired in radar geometry are employed. Aligning with the Sentinel-1 UTM zone, the desired Coordinate Reference System (CRS) is established. Within this framework, the operator has the flexibility to designate both the desired pixel spacing in the new CRS and the preferred method of image resampling. This processing stage also enables the spatial

alignment of Sentinel-1 GRD products, thereby facilitating the geolocation of data onto a unified spatial grid. This strategic step fosters the utilization of satellite virtual constellations.

The SNAP software uses the cluster analysis method to categorize Sentinel-1 data without supervision. Started by loading the Sentinel-1 data into SNAP and filtering and calibrating it beforehand then, a subset of the previously processed data was produced for use. They selected the cluster analysis algorithm from the list of SNAP possibilities and adjusted the parameters to suit the requirements. The parameters included the clustering technique and the number of clusters that would be created. Executed the cluster analysis method on the subset of data once the settings were established. As a result, various clusters within the data emerged based on their similarity to one another. The clusters were visualized using SNAP built-in visualization capabilities and validated to ensure they were correct and relevant to the study.

The application of the Random Forest algorithm within the SNAP software facilitated the utilization of a supervised classification approach on Sentinel-1 data. This procedural strategy aimed to categorize diverse land cover classifications within a specified region of interest (De Luca et al., 2022; Valdivieso-Ros et al., 2023). Table 2 illustrates the categorization employed in the research. To enhance image quality and minimize interference, a sequence of pre-processing steps was applied to the Sentinel-1 data. Radiometric alignment, multi-looking procedures, speckle reduction techniques, and terrain adjustments comprised the pre-processing phase. Following these preparatory measures, the data stood primed for the classification phase. Harnessing the Random Forest algorithm, a prevalent machine learning tool for classification tasks, the algorithm underwent training using a selection of training samples extracted from the study vicinity. These training samples were meticulously categorized to align with distinctive land cover categories. Employing the trained Random Forest algorithm, the classification endeavour unfolded, culminating in the organization of Sentinel-1 data into discrete land cover classes. The assessment of classification accuracy ensued through a confusion matrix, presenting insights into accurately and erroneously classified pixels. The outcomes of the classification process underscored the efficacy of the Random Forest algorithm in catego-

Table 2. Categorization framework employed in the study.

Urban	Includes built-up areas like residential, industrial, and commercial areas except for roads
Waterbody	Includes lakes, ponds, and rivers
Paddy field	Includes flooded fields of arable land used for growing semiaquatic crops, most notably rice and taro.
Vegetation	Includes agricultural croplands

rizing diverse land cover types within the research area. This was highlighted by the notable accuracy achieved in the overall classification, emphasizing the algorithm’s proficiency in this context.

Various techniques for filtering and processing were employed to mitigate the effects of speckle divergence and enhance the caliber of radar imagery utilized in urban cartography (Hyypä et al., 2015). The SNAP application was employed to execute supervised classification on Sentinel-1 data through the utilization of the random forest methodology in the presence of speckle divergence (Fiorillo et al., 2020; Tavares et al., 2019). Filtering methodologies were deployed to eradicate noise and speckle artifacts from the dataset. The classification task was conducted utilizing a training dataset containing instances representing diverse land cover categories. Using the speckle divergence metrics of individual pixels within the Sentinel-1 dataset, the system underwent training to effectively categorize them into distinct land cover classes.

Employing the random forest algorithm and speckle divergence within the framework of the SNAP emerged as a highly effective approach for cartographic land cover delineation using Sentinel-1 data. The outcomes yielded high precision and imparted valuable insights applicable to land administration and surveillance purposes.

2.4. GIS Environment and Accuracy

Two separate collections of measurements were employed to evaluate precision. The initial phase encompassed the compilation of 30 training locations, with 20 designated for instructing the supervised classifier and the remaining 10 reserved for cross-validation through Google Earth imagery. To substantiate the urban footprint delineation of both SAR and Google Earth data, 150 authentic reference points were amassed and uniformly spread across the chosen study area as the secondary metric for assessing accuracy. Redefining the combined SAR data within the context of GIS parameters enabled the quantitative cartographic representation of urbanization shifts. The transformation involved changing integer values to convert floating point information into

a vectorised structure. Utilizing the algorithm of natural breaks classification, the vector-based stratum underwent segmentation into diverse categories. Subsequently, the classification segment was overlaid onto a foundational map to evaluate alterations within the urban landscape (Harikumar et al., 2012; Schultz and Engman, 2012).

3. RESULTS AND DISCUSSION

Sentinel-1 data, encompassing SAR imagery, has proven efficacious in the continuous monitoring and analysis of urban sprawl. The study area exemplifies an urban landscape, comprising roadways, edifices, sparse greenery, arboreal elements, and a diverse array of features spanning a broader spectral spectrum. These attributes necessitate systematic categorization, entailing the compilation of distinct spectral signatures indispensable for this research endeavour. This meticulous approach is imperative due to the resampled spatial resolution of the multi spectral imagery being 10 meters. Employing a mean reduction technique, the Sentinel-1 images, pivotal to the study, were procured from image repositories corresponding to the 2015 and 2023 periods of interest. These Sentinel-1 images, showcased through the 'VV', 'VH', and 'VV' bands, were mapped onto the red, green, and blue colour channels, sequentially. Evidently, urban sectors manifest heightened backscatter in the 'VV' band. To facilitate image classification and ensure accuracy, training, and validation samples were derived from high-resolution imagery of the study area. The assortment of these samples from both Sentinel-1 data and Google Earth images from the years 2015 and 2023 respectively is integral to the process of classification and precision assessment.

The utilization of speckle divergence analysis facilitates a more effective differentiation of settlement regions and their attributes compared to reliance solely on intensity imagery (Fig. 2). Notably, the application of speckle divergence analysis enhances the visual clarity and luminosity of settlement areas. Consequently, this outcome was subsequently harnessed to advance the classification of settlements in

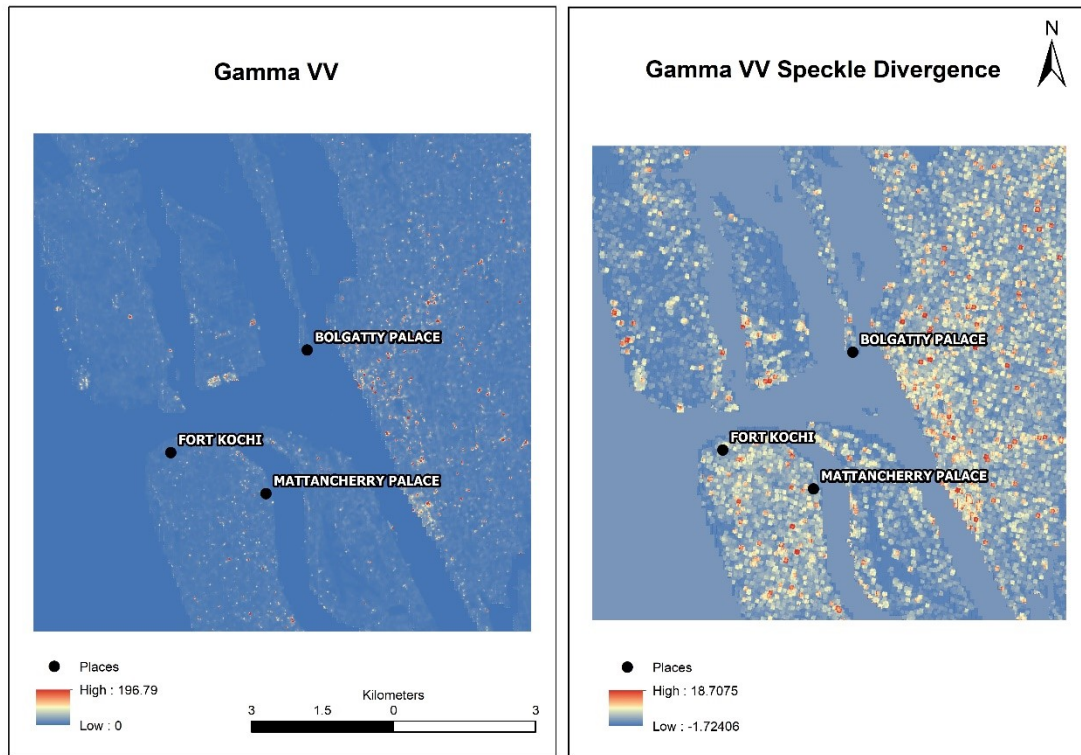


Fig. 2. Comparison of pre-processing approaches on VV bands of SAR data (a) Gamma VV (2015) (b) Gamma VV Speckle Divergence (2023).

conjunction with Sentinel-1 imagery. A texture representation emerges from the localized speckle characteristics present in the SAR intensity information. The divergence in the speckle pattern approach capitalizes on the contrast between the heterogeneity observed in local images and the anticipated scene-specific heterogeneity of the well-defined speckle pattern. This method operates under the presumption that when a resolution cell contains a greater number of actual structures, the deviation at a local level from the meticulously generated speckle (Baydogan and Sarp, 2022; Dekker et al., 2011; Jiang et al., 2020).

4. CONCLUSION

The GCDA was taken as a case study representing a swiftly expanding urban area. Detecting the urban footprint was effectively examined by employing diverse classifiers on a variety of remote sensing data, encompassing Google Earth and microwave information. The model has achieved an optimal classification count and has displayed stability, as evidenced by the minor deviations in class sensitivity analysis. Consequently, any potential increase in

the number of classes will not yield substantial alterations in the percentage shift. To pinpoint the spectral characteristics of the classes encompassed within the designated study vicinity and utilize them as reference sites for supervised classification decision trees, it is essential to first determine the most stable number of classes from the unsupervised classification. The outcomes of the present research underscore the imperative of synergizing microwave and optical remote sensing data to attain precise urban footprint mapping. Illustratively, the urban footprint of the GCDA was proficiently charted by employing the yellow range thresholds of the consolidated stacked layer. This case serves as an example of an urbanized coastal municipality with limited vegetative covering. Notably, urban elements exhibit higher brightness in comparison to other land use categories due to VV speckle divergence. Furthermore, the exceptional spatial resolution of the Sentinel-1A image enabled the identification of intricate details down to the building level utilizing the applied methodology. Identifying urban zones is now facilitated, particularly owing to the backscatter originating from vertical structures such as building areas and rooftops.

References

- Alharthi, A., El-Sheikh, M.A., Elhag, M., Alatar, A.A., Abadi, G.A., Abdel-Salam, E.M., Arif, I.A., Baeshen, A.A., Eid, E.M., 2020. Remote sensing of 10 years changes in the vegetation cover of the northwestern coastal land of Red Sea, Saudi Arabia. *Saudi Journal of Biological Sciences* 27(11), 3169–3179. <https://doi.org/10.1016/j.sjbs.2020.07.021>.
- Bahrawi, J., Ewea, H., Kamis, A., Elhag, M., 2020. Potential flood risk due to urbanization expansion in arid environments, Saudi Arabia. *Natural Hazards* 104, 795–809. <https://doi.org/10.1007/s11069-020-04190-7>.
- Baydogan, E., Sarp, G., 2022. Urban footprint detection from night light, optical and SAR imageries: A comparison study. *Remote Sensing Applications: Society and Environment* 27, 100775. <https://doi.org/10.1016/j.rsase.2022.100775>.
- De Luca, G., Silva, M.N., J., DiFazio, S., Modica, G., 2022. Integrated use of Sentinel-1 and Sentinel-2 data and open-source machine learning algorithms for land cover mapping in a Mediterranean region. *European Journal of Remote Sensing* 55(1), 52–70. <https://doi.org/10.1080/22797254.2021.2018667>.
- Dekker, A.G., Phinn, S.R., Anstee, J., Bissett, P., Brando, V.E., Casey, B., Fearn, P., Hedley, J., Klonowski, W., Lee, Z.P., 2011. Intercomparison of shallow water bathymetry, hydro-optics, and benthos mapping techniques in Australian and Caribbean coastal environments. *Limnology and Oceanography: Methods* 9(9), 396–425. <https://doi.org/10.4319/lom.2011.9.396>.
- Elhag, M., Psilovikos, A., Sakellariou-Makrantonaki, M., 2013. Land use changes and its impacts on water resources in Nile Delta region using remote sensing techniques. *Environment, development and sustainability* 15, 1189–1204. <https://doi.org/10.1007/s10668-013-9433-5>.
- Esch, T., Thiel, M., Schenk, A., Roth, A., Muller, A., Dech, S., 2009. Delineation of urban footprints from TerraSAR-X data by analyzing speckle characteristics and intensity information. *IEEE Transactions on Geoscience and Remote Sensing* 48(2), 905–916. <https://doi.org/10.1109/TGRS.2009.2037144>.
- Fiorillo, E., Giuseppe, E., Fontanelli, G., Maselli, F., 2020. Lowland rice mapping in Sédhiou Region (Senegal) using sentinel 1 and sentinel 2 data and random forest. *Remote Sensing* 12(20), 3403. <https://doi.org/10.3390/rs12203403>.
- Harikumar, V., Joshi, M., Raval, M., Gajjar, P.P., 2012. Conference 8537: Image and Signal Processing for Remote Sensing. *Remote Sensing* 107. URL: <https://citeseerx.ist.psu.edu/document?repid=rep1&type=pdf&doi=81efaf634ffe9de18859fb1db3b451f064fae6d0#page=107>.
- Hyypä, J., Karjalainen, M., Liang, X., Jaakkola, A., Yu, X., Wulder, M., Hollaus, M., White, J.C., Vastaranta, M., Karila, K., 2015. *Remote sensing of forests from Lidar and Radar, Land Resources Monitoring, Modeling, and Mapping with Remote Sensing*. CRC Press Boca Raton, FL, USA. <https://doi.org/10.1201/b19322>.
- Jiang, M., Hooper, A., Tian, X., Xu, J., Chen, S.N., Ma, Z.F., Cheng, X., 2020. Delineation of built-up land change from SAR stack by analysing the coefficient of variation. *ISPRS Journal of Photogrammetry and Remote Sensing* 169, 93–108. <https://doi.org/10.1016/j.isprsjprs.2020.08.023>.
- Li, Q., Zheng, B., Tu, B., Yang, Y., Wang, Z., Jiang, W., Yao, K., Yang, J., 2020. Refining urban built-up area via multi-source data fusion for the analysis of dongting lake eco-economic zone spatiotemporal expansion. *Remote Sensing* 12(11), 1797. <https://doi.org/10.3390/rs12111797>.
- Massonnet, D., Feigl, K.L., 1998. Radar interferometry and its application to changes in the Earth's surface. *Reviews of Geophysics* 36(4), 441–500. <https://doi.org/10.1029/97RG03139>.
- May, M., Jose, P.T., 2009. *Environmentally-Efficient Development Management System for Greater Kochi in Kerala State*. Unpublished PhD thesis. Cochin University of Science And Technology, India. URL: <https://dyuthi.cusat.ac.in/xmlui/handle/purl/3839>.
- Prakash, A., Diksha, Kumar, A., 2023. Measuring Vertical Urban Growth of Patna Urban Agglomeration Using Persistent Scatterer Interferometry SAR (PSInSAR) Remote Sensing. *Remote Sensing* 15(14), 3687. <https://doi.org/10.3390/rs15143687>.
- Satheendran, S.S., Chandran, S.S., Mathew, J.C., 2022. The Evolution of Lighting in South-West India from Night-Time Lights: 2012–2020. *Spatial Information Research* 30(2), 261–277. <https://doi.org/10.1007/s41324-021-00428-z>.
- Schultz, G.A., Engman, E.T., 2012. *Remote sensing in hydrology and water management*. Springer Science & Business Media. <https://doi.org/10.1007/978-3-642-59583-7>.
- Schumm, S.A., 1979. Geomorphic thresholds: the concept and its applications. *Transactions of the Institute of British Geographers* , 485–515 <https://doi.org/10.2307/622211>.
- Shreekumar, S., Madhu, D., Akella, A.K., 2021. *Urban Flood Susceptibility Mapping of Kochi Taluk Using Remote Sensing and GIS, 2021 Fourth International Conference on Electrical, Computer and Communication Technologies (ICECCT)*. IEEE. URL: <https://ieeexplore.ieee.org/abstract/document/9616790>.
- Taubenböck, H., Esch, T., Felber, A., Wiesner, M., Roth, A., Dech, S., 2012. Monitoring urbanization in mega cities from space. *Remote sensing of Environment* 117, 162–176. <https://doi.org/10.1016/j.rse.2011.09.015>.
- Tavares, P.A., Beltrão, N.E.S., Guimarães, U.S., Teodoro, A.C., 2019. Integration of sentinel-1 and sentinel-2 for classification and LULC mapping in the urban area of Belém, eastern Brazilian Amazon. *Sensors* 19(5), 1140. <https://doi.org/10.3390/s19051140>.
- Thiel, M., Esch, T., Schenk, A., 2008. *Object-oriented detection of urban areas from TerraSAR-X data, Proceeding of ISPRS 2008 Congress (37), Part B*. Citeseer. URL: <https://citeseerx.ist.psu.edu/document?repid=rep1&type=pdf&doi=a0f5902027f122e24bec51408e1a37bbb4914d4b>.
- Thomas, G., Sherin, A., Ansar, S., Zachariah, E., 2014. Analysis of urban heat island in Kochi, India, using a modified local climate zone classification. *Procedia Environmental Sciences* 21, 3–13. <https://doi.org/10.1016/j.proenv.2014.09.002>.
- Valdivieso-Ros, C., Alonso-Sarria, F., Gomariz-Castillo, F., 2023. Effect of the Synergetic Use of Sentinel-1, Sentinel-2, LiDAR and Derived Data in Land Cover Classification

- of a Semiarid Mediterranean Area Using Machine Learning Algorithms. *Remote Sensing* 15(2), 312. <https://doi.org/10.3390/rs15020312>.
- Wang, C., Wang, X.S., Xu, Y., Zhang, B., Jiang, M., Xiong, S., Zhang, Q., Li, W., Li, Q., 2022. A new likelihood function for consistent phase series estimation in distributed scatterer interferometry. *IEEE Transactions on Geoscience and Remote Sensing* 60, 1–14. <https://doi.org/10.1109/TGRS.2022.3170567>.
- Wang, J., Qu, S., Peng, K., Feng, Y., 2019. Quantifying urban sprawl and its driving forces in China. *Discrete Dynamics in Nature and Society*, 1–14 <https://doi.org/10.1038/s41377-019-0210-6>.
- Yamaguchi, Y., Moriyama, T., Ishido, M., Yamada, H., 2005. Four-component scattering model for polarimetric SAR image decomposition. *IEEE Transactions on Geoscience and Remote Sensing* 43(8), 1699–1706. <https://doi.org/10.1109/TGRS.2005.852084>.